



SIMULATION OF FLOW IN A CENTRIFUGAL PUMP OF ESP SYSTEMS USING COMPUTATIONAL FLUID DYNAMICS

^aMaitelli, C. W. S. de P.¹; ^bBezerra, V. M. de F.; ^cda Mata, W.

^aLaboratório de Automação em Petróleo - LAUT, Centro de Tecnologia, Universidade Federal do Rio Grande do Norte, Campus Universitário, Lagoa Nova, CEP 59072-970, Natal/RN/Brasil.

^bDepartamento de Engenharia Química, Universidade Federal do Rio Grande Do Norte.

^cDepartamento de Engenharia de Petróleo, Universidade Federal do Rio Grande do Norte.

ABSTRACT

Artificial lift methods can be implemented in the oil industry in order to increase the production rate of flowing oil or gas wells. Electrical Submersible Pumping (ESP) is a complex and viable method of artificial lift that is applicable to a wide range of flow rates. ESP systems are responsible for the highest amount of total fluids produced by any artificial lift method. This paper presents a 3D simulation of the stationary flow in the impeller and stator of a mixed centrifugal pump using Computational Fluid Dynamics (CFD) techniques and a commercial software, ANSYS® CFX® Release 11.0. Three conditions were simulated to obtain the pressure fields in the impeller and stator in a stage of the pump. Comparisons among the simulations of the present work and the head capacity of the performance curve given by pump manufacturer were performed and showed satisfactory agreement.

KEYWORDS

Centrifugal pumps; numerical simulation; ESP systems; Computational Fluid Dynamics (CFD); performance curves.

¹ To whom all correspondence should be addressed.

Address: | Telephone/Fax number: (55) 84 3215-3940 / (55) 84 3215-3940 | e-mail: maitelli@ufrnet.br

1. INTRODUCTION

The difficulties to install, to maintain and to keep equipments in operation are factors that burden the petroleum production in high depths, requiring the development of new technologies and methods to reduce the failures in the subsurface equipment. The choice of the artificial lift method depends on parameters such as the geometry and characteristics of the reservoir, fluids properties, equipment availability and generation of energy. The evolution of the design and manufacture of equipments in recent years has rendered the Electrical Submersible Pumping (ESP) an appropriate solution to lift large volumes of fluid both onshore and offshore, in adverse conditions of temperature and viscous fluids (Thomas, 2001). In spite of the difficulties in the use of this method when in the presence of sand, high gas liquid ratio (GLR) and high bottom hole temperatures, ESP is one of the most used and versatile methods of artificial lift in the world.

A typical electrical submersible pumping system installation is comprised of an electric motor, seal section, gas separator, multi-stage centrifugal pump and electric power cable. All this set runs into the well, protected by the casing. On the surface, the main components are the cable junction box, switchboard, motor controller and transformers. The centrifugal pumps are the heart of the system and are used in the ESP systems add power to the fluid to lift it toward the surface. The centrifugal pumps are composed of two main parts: an impeller (rotor) that rotates at the motor speed and imparts centrifugal forces to the production fluids and the diffuser (stator), which is the fixed part that guides the flow to the discharge.

The theoretical treatment of the flow through hydraulic machines is difficult due to factors such as irregular sections in the curved passages path, for instance. The impeller's channels are in a circular motion and the simple and idealized relations established in hydraulics, if applied directly to such flow, may give incorrect quantitative answers and false flow patterns (Stepanoff, 1957). In order to overcome this problem, for many years, some authors have studied single phase flow in the centrifugal pumps using computational models (Pérez et al., 2006; Zhou et al., 2006; Anagnostopoulos, 2006; Asuaje, 2005; Asuaje, 2003; van Esch, 1997).

This work presents a numerical simulation of a single phase three-dimensional flow in a centrifugal pump used in ESP systems. To accomplish this task the geometry of a known centrifugal pump was developed. The simulations have been carried out using CFD techniques and a commercial software based on the finite volume method, ANSYS® CFX® Release 11.0. The results of the simulations include the pressure fields obtained to the internal flow in the impeller and diffuser channels. The main objectives were to verify the effect of the interaction between the pump impeller and diffuser and to compare the results with the head performance curve published by the pump manufacturer. Three conditions were tested for the calculation of the pressures and the total head: the first condition was the impeller simulation with the blades length equivalent to the real model (C1); the second option was tested for the condition of complete connection of pump, impeller and diffuser, with the real blades length (C2); in the third option (C3), the impeller and the diffuser had their external radii increased by four (4) mm.

2. MATERIALS AND METHODS

2.1 Geometry

The centrifugal pump operation is very simple. Basically, energy is added to the fluid resulting in work. Pumps can be manufactured with many diameters and the design of submersible centrifugal pumps fall into two general categories, in agreement with the capacity to be pumped. The smaller flow pumps are generally of radial flow design and in the larger diameter pumps, the design changes to a mixed flow. In this case the stage design imparts a direction to the fluid that contains substantial axial direction as well as radial direction. ESP pumps can be applicable to a wide range of flow rates from a few hundred up to around 100.000 bpd. The model developed in this study is based on the FC-2700 pump of the CENTRILIFT 400 series. The geometric characteristics were determined through manual inspection with digital pachymeter and drawn in the software AUTOCAD® release 2006, following mechanical drawing norms.

Figure 1 presents the three-dimensional pump geometry obtained for each stage. In Figure 2, the meridional profiles of the diffuser and the impeller

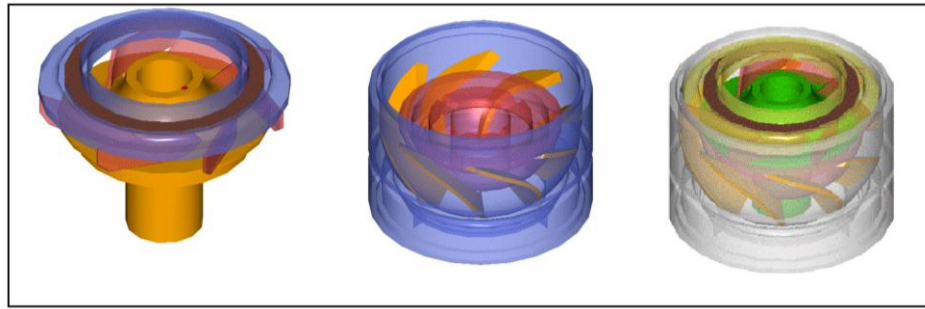


Figure 1. 3D/CAD drawing of the impeller, diffuser, entire pump (impeller and diffuser), from left to right.

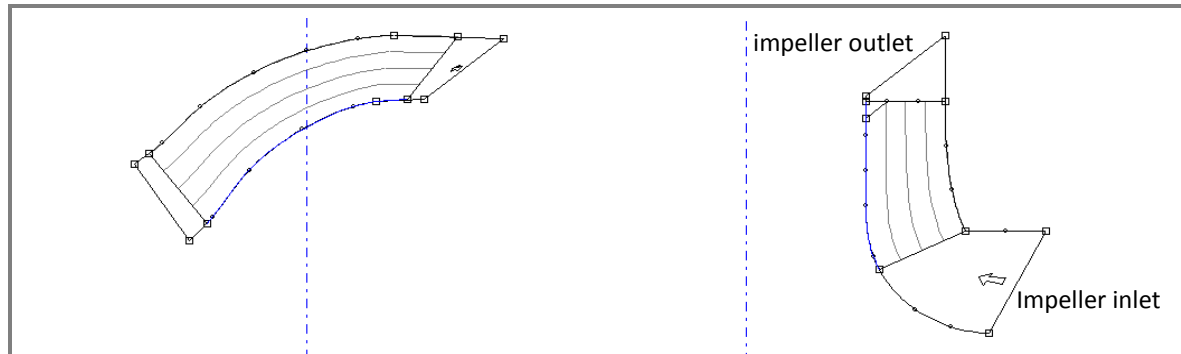


Figure 2. Meridional profiles of diffuser and impeller, modeled in BladeGen/ANSYS® CFX® 11.0.

showing their channels in two dimensions are depicted. They were obtained with the BladeGen - ANSYS® CFX® 11.0, which is a blade geometry design tool. The geometry was simplified in order to comply with the requirements and limitations of the program. Table 1 gives the main parameters and pump geometric characteristics.

Table 1. Pump geometric characteristics.

Characteristics	Value
impeller inlet radius (mm)	18.28
impeller outlet radius (mm)	38.39
impeller inlet blade angle	30.89°
impeller outlet blade angle	41.72°
impeller inlet height (mm)	10.82
impeller outlet height (mm)	8.66
total impeller height (mm)	60.09
total diffuser height (mm)	57.92
total height, impeller and diffuser (mm)	63.50
diffuser external diameter (mm)	88.3
impeller blades number	07
diffuser blades number	08

2.2 Mathematical model

The three-dimensional and incompressible flow in the pumps can be described with the conservations laws of movement and mass in cylindrical coordinates for radial (r), angular (θ) and axial (z) directions. In terms of the divergence theorem, the continuity equation or conservation mass, for a newtonian fluid in steady state can be written as:

$$\nabla \cdot \vec{V} = 0 \quad (1)$$

and the momentum equation is:

$$\rho \left[\vec{V} \cdot \left(\nabla \vec{V} \right) \right] = -\nabla p + \mu_{ef} \left(\nabla^2 \vec{V} \right) + \vec{F} \quad (2)$$

where:

ρ = fluid density

\vec{V} = absolute velocity vector

μ_{ef} = fluid effective viscosity

p = pressure

\vec{F} = body forces

The left side term in Equation (2) represents the convective acceleration. The right side terms represent the pressure gradient, the viscous effects and the source terms respectively. The turbulence model chosen was the $k-\varepsilon$ model due to its stability, widespread application in commercial softwares and robustness. The $k-\varepsilon$ model and its extensions resolve the partial differential equations for turbulent kinetic energy k and the dissipation rate ε as shown by the Equations (3) and (4):

$$\rho \left[\vec{V} \cdot (\nabla k) \right] = \nabla \cdot (\Gamma_c \nabla k) + P - \rho \varepsilon \quad (3)$$

$$\rho \left[\vec{V} \cdot (\nabla \varepsilon) \right] = \nabla \cdot (\Gamma_\varepsilon \nabla \varepsilon) + C_{\varepsilon 1} \frac{\varepsilon P}{k} - C_{\varepsilon 2} \frac{\rho \varepsilon^2}{k} \quad (4)$$

The diffusion coefficients are:

$$\Gamma_c = \mu + \frac{\mu_t}{\sigma_k} \quad (5)$$

$$\Gamma_\varepsilon = \mu + \frac{\mu_t}{\sigma_\varepsilon} \quad (6)$$

The terms $C_{\varepsilon 1}$, $C_{\varepsilon 2}$, σ_k e σ_ε in the Equations (3) and (4) are typical constants in the $k-\varepsilon$ turbulence model and their values are:

$$C_{\varepsilon 1} = 1.44; C_{\varepsilon 2} = 1.92; \sigma_k = 1.0 \text{ e } \sigma_\varepsilon = 1.3$$

P is the generation rate of turbulent kinetic energy, and can be calculated with the expression:

$$P = \mu_{ef} \Phi \quad (7)$$

also,

$$\mu_{ef} = \mu + \mu_t \quad (8)$$

and

$$\mu_t = C_\mu \rho \frac{k^2}{\varepsilon} \quad (9)$$

where:

Φ = dissipation viscous rate in cylindrical coordinates

μ = molecular viscosity

μ_t = turbulent viscosity

$C_\mu = 0.09$, a constant

All the previous equations are valid both for the impeller and for the diffuser, however the rotational forces in the source terms will only apply for the impeller in the movement equation as a result of Coriolis forces and centrifugal forces.

2.3 Simulation parameters, discretization, boundary conditions

The three-dimensional flow simulations were performed in the commercial software, based on CFD techniques, ANSYS® CFX® release 11.0. Water was the single phase fluid chosen in this study, at standard conditions, with density equals 1000 kg/m³. The impeller rotational speed was set at 3500 rpm. For each condition (C1, C2 e C3), ten (10) flow rates were simulated.

The selected convergence criteria of mass equations were maximum residual of 0.0001 for root-mean-square (RMS). All the simulations were carried out in a computer with Intel(R) Core (TM)2

Quad processor, with a 3.0-GHz CPU and 8.0 Gb of RAM. Due to computational limitations, software characteristics and problem symmetry, in the problem domain, just one passage (or channel) was modeled in the impeller and diffuser. The meshes were generated by ANSYS® CFX® 11.0 with wedge elements, pyramid elements and tetrahedral elements in a non-structured mesh, which is more appropriate to discretize irregular geometries (Maliska, 2004). The choice for the interface between the impeller and the diffuser was frozen rotor, typical for turbomachines in ANSYS® CFX® 11.0, specific for the steady state flow regime and composed structures with a rotative part (the impeller) and a fixed part (the diffuser) (Ansys CFX Reference Guide, 2006). The reference pressure in all cases was adjusted to one (1) atm.

The boundary conditions were set as follows: a total uniform pressure of one (1) atm at inlet and variable mass flow rate at outlet. These choices have resulted in robust and right solutions in the scope of the computational tool utilized (Ansys CFX - Solver Modeling Guide, 2006). Periodicity conditions were adjusted due to problem symmetry and solid walls not crossing the fluids were set for each run. The summary of boundary conditions and simulation parameters are shown in Table 2.

3. RESULTS AND DISCUSSION

3.1 Simulation of the SAGD process in conventional model

Figure 3 shows the results obtained with the simulations for the head characteristic curves (head versus flow rate) for the three conditions tested (C1, C2 e C3), compared with the manufacturer's data.

The curves obtained from CFD model show a same tendency of behavior for the three cases in study. This tendency was compared with manufacturer experimental curve. For the first condition (C1), the simulation was carried out with the impeller, without considering the diffuser for the numerical analysis. It can be observed that, for the smallest flow rates, there occurs an excessive head increase. This phenomenon happens because the diffuser is not considered in the simulation. The

interaction between the two components in the pump stage (impeller plus diffuser) must generate friction losses mainly in the case of smallest flow rates.

For C2 and C3, conditions of the impeller coupled with the diffuser, an identical tendency to the experimental curve was verified. In the C2 condition, in spite of the same behavior if compared with the manufacturer curve, large losses occur due to the coupling with the diffuser will occur. This fact is associated to geometric simplifications established to allow the coupling between the impeller and the diffuser, besides physical and numerical reasons such as convergence problems, flow instabilities and recirculation problems. To overcome such difficulties, the C3 condition was investigated, with the blades extended by four (4) mm obtaining better results if compared with the manufacturer head curve. Figures 4 to 9 show the meridional profiles of the impeller and the diffuser channels for C1, C2 and C3. The figures show the pressure profiles when the volumetric flow rate is 2500 bpd.

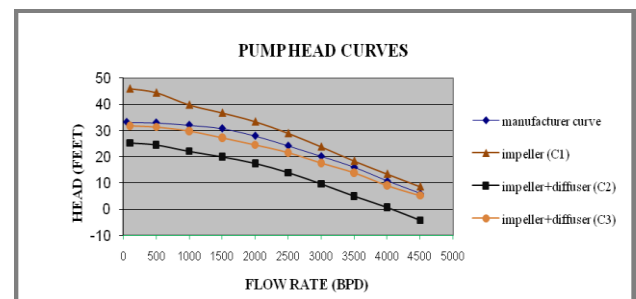


Figure 3. Results obtained in the simulations and manufacturer head curve.

The pressure in C1 and C2 conditions were identical in the impeller outlet. For the values of pressure obtained in the outlet impeller and in the diffuser entrance (C2 e C3) the values of pressure are continuous at the interface. This fact is an evidence of the interaction between the two structures and their meshes: the rotative impeller and the fixed diffuser.

Table 2. Simulation parameters and boundary conditions.

SIMULATION PARAMETERS	BOUNDARY CONDITIONS / CFX VALUES		
	IMPELLER (C1)	IMPELLER+DIFFUSER (C2)	IMPELLER+DIFFUSER (C3)
Simulation domain	An impeller channel with real measurements for the blades	Impeller + diffuser, one channel, real measurements	Impeller + diffuser, one channel, extended blade
Fluid	Water at standard conditions	Water at standard conditions	Water at standard conditions
Mesh	Non-structured; 90615 elements for the impeller	Non-structured; 90615 elements for the impeller and 148177 elements for the diffuser	Non-structured; 155084 elements for the impeller and 152507 elements for the diffuser
Inlet total pressure	1 atm	1 atm	1 atm
Outlet mass flow rate	Variable (kg/s)	Variable (kg/s)	Variable (kg/s)
Slip in the walls	No slip	No slip	No slip
Turbulence model	$k - \varepsilon$	$k - \varepsilon$	$k - \varepsilon$
Flow regime	Steady state	Steady state	Steady state
Rotational speed	3500 rpm	3500 rpm	3500 rpm
Periodicity	Symmetrical surfaces in the middle of the channel between two blades	Symmetrical surfaces in the middle of the channel between two blades	Symmetrical surfaces in the middle of the channel between two blades
Walls	Solid walls not crossing the fluid	Solid walls not crossing the fluid	Solid walls not crossing the fluid
Impeller/diffuser interface	–	Frozen rotor	Frozen rotor

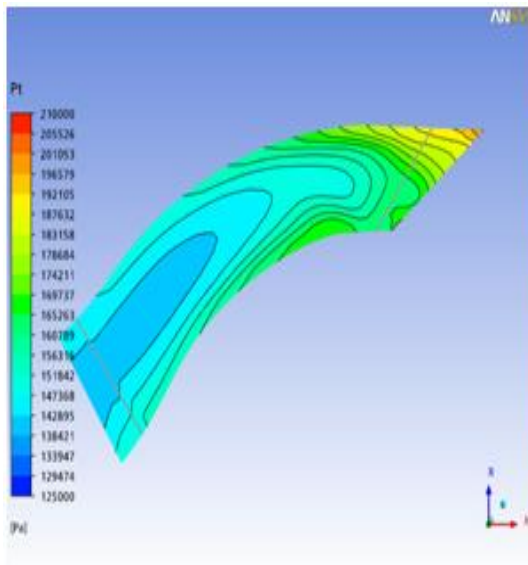


Figure 4. Pressure in the diffuser channel (C2)

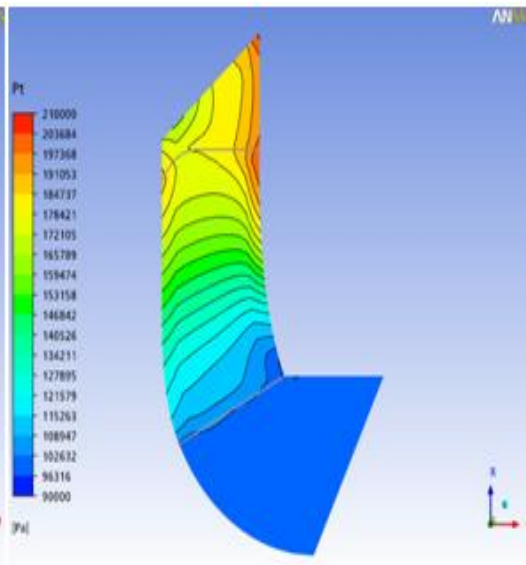


Figure 5. Pressure in the impeller channel (C1 e C2)

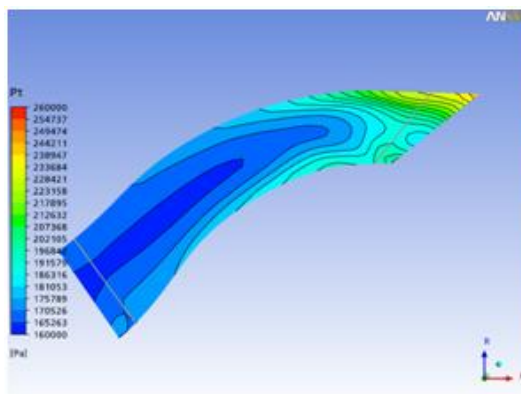


Figure 6. Pressure in the diffuser channel (C3)

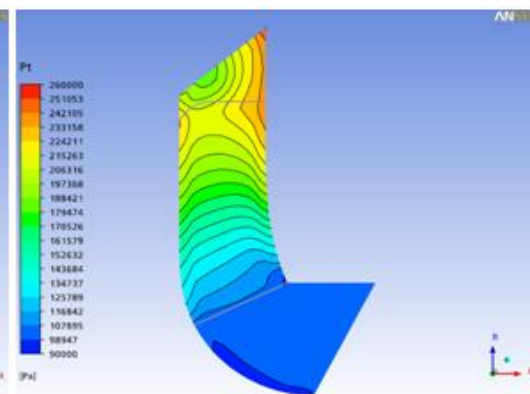


Figure 7. Pressure in the impeller (C3)

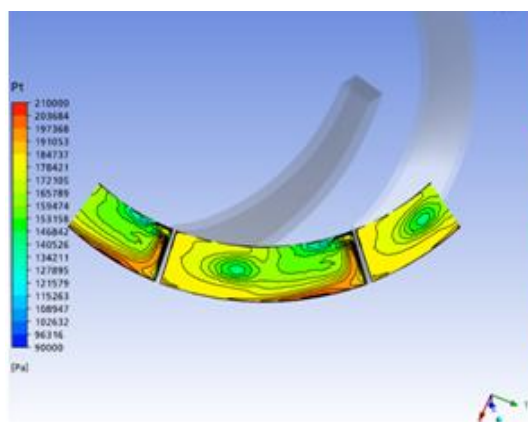


Figure 8. Pressure in the diffuser inlet (C2)

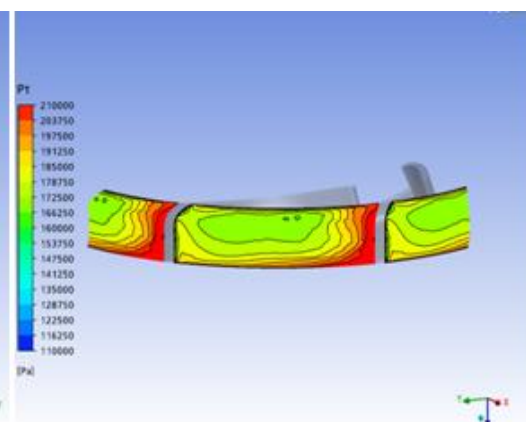


Figure 9. Pressure in the outlet impeller (C2)

4. CONCLUSIONS

In this paper a computational simulation of the centrifugal pump internal flow was implemented. A CFD code, the ANSYS® CFX® 11.0, was used to obtain the head performance curve and to evaluate the interface connection between the pump parts: the impeller and the diffuser. Boundary conditions were adjusted in the software to characterize the three-dimensional problem. Although the simplifications were done in the model, in order to adjust the geometry to the software limitations, numerical analysis using a CFD code, ANSYS® CFX® 11.0 presents results in agreement with the references. The results obtained for the pressure fields, and therefore to the head performance curve, were satisfactory in the three conditions tested.

In the C1 condition, high values were obtained for the head curve, comparing to the manufacturer experimental curve. In this case, there is no influence from the diffuser, so the friction losses are smaller, affecting the pressure fields and increasing the head values. This fact represents the necessity to introduce the friction losses due to coupling between the diffuser and impeller. Another factor that increases the head values is that, for smaller flow rates values, closed to zero (0), the simulation convergence is more difficult.

In the C2 and C3 conditions, simulations were performed with the entire pump and diffuser coupled to the impeller. For the two situations, the pressure in the impeller channels increases from the entrance to the discharge in successive ranges. This fact shows the energy transfer in the impeller (Figures 5 and 7). In the impeller outlet, a reduction in the pressure values is observed (Figures 5 and 7). This occurs due to the friction losses, recirculation of fluids and the conditions of coupling used by the software. This actually means that fluid displacement occurs due to the rotational movement of the fluid. The losses at the interface between the impeller and the diffuser can be noticed in C2 and C3 conditions. To minimize the losses, C3 condition is more adequate to describe the problem. The boundary conditions of total pressure at inlet and mass flow at outlet satisfy the problem convergence. Another factor to be reviewed is that the use of only one channel for the impeller and one for the diffuser did not affect

negatively the simulations and the use of BladeGen - ANSYS® CFX® 11.0 tool proved to be an appropriate solution in defining the geometry of the problem, in spite of the simplifications made.

In future investigations, viscous fluids and two-phase flow must be considered to provide a better interpretation of questions involving the losses in ESP systems, besides gas locking and surging problems that can block the fluid entrance in the stage, decreasing the pump efficiency and damaging the equipments of the system.

ACKNOWLEDGEMENTS

This research was supported by project AUTOPOC/UFRN/PETROBRAS and the Programa de Pós-Graduação em Ciência e Engenharia de Petróleo/PPgCEP/UFRN. It was developed in the Laboratório de Automação em Petróleo (LAUT/UFRN). The authors are thankful the team of project AUTOPOC.

5. REFERENCES

- Anagnostopoulos, J. S. Numerical calculation of the flow in a centrifugal pump impeller using cartesian grid. In: 2nd Wseas Int. Conference on Applied and Theoretical Mechanics, 2006, Veneza, Itália, **Proceedings 2nd WSEAS**, Veneza, 2006, p. 124-129. Available at: <http://www.fluid.mech.ntua.gr/lht/PYTHAGORAS/dimosieuseis/D-9.pdf>.
- ANSYS CFX - Reference Guide, ANSYS CFX Release 11.0. United States, December, 2006, Software handbook, 934p.
- ANSYS CFX - Solver Modeling Guide, ANSYS CFX Release 11.0. United States, December, 2006, Software handbook, 566p.
- Asuaje, M. et al. Numerical modelization of the flow in centrifugal pump: volute influence in velocity and pressure fields, **International Journal of Rotating Machinery**, 2005:3, p. 244-255, 2005. Available at: <http://www.hindawi.com/journals/ijrm/2005/345857.abs.html>

Asuaje, M. **Méthodologie et optimisation dans la conception et l'analyse des performances des turbomachines à fluide incompressible**, 101f.

Thèse de Doctorat. Ecole Nationale Supérieure d'Arts et Métiers - Centre de Paris, Paris, 2003. (in French). Available at: <http://tel.archives-ouvertes.fr/docs/00/04/66/74/PDF/tel-00005730.pdf>

MALISKA, C. R. **Transferência de calor e mecânica dos fluidos computacional**. Rio de Janeiro: LTC - Livros Técnicos e Científicos Editora S.A., 2ª edição, 2004. 453p. (In Portuguese).

Pérez, J. L.; Carrilo L. P.; Espinoza H. Three-dimensional simulation of the entrance-impeller interaction of a hydraulic disc pump, **Rev. Téc. Ing. Univ. Zulia**, v. 29, n. 1, p. 49-57, 2006. Available at: http://www.scielo.org.ve/scielo.php?script=sci_arttext&pid=S025407702006000100007&lng=es&nr_m=iso&tlng=es.

STEPANOFF, A. J. **Centrifugal and axial flow pumps, theory, design and application**. Malabar:

Krieger Publishing Company, 2nd edition, 1957. 462p. (In English).

THOMAS, J. E. **Fundamentos da engenharia de petróleo**. Rio de Janeiro: Editora Interciência, 2ª edição, 2001. 271p. (In Portuguese).

van ESCH, B. P. M. **Simulation of three-dimensional unsteady flow in hydraulic pumps**, 76p, Doctoral Thesis. University of Twente, Enschede, Netherlands, 1997. (In English). Available at: <http://www.thw.ctw.utwente.nl/research/PhD-theses/Van%20Esch.pdf>.

Zhou W., Zhao Z.; Lee T. S., Winoto S. H. Investigation of flow through centrifugal pump impellers using computational fluid dynamics, **International Journal of Rotating Machinery**, 9(1): p. 49-61, 2003. Available at: <http://downloads.hindawi.com/journals/ijrm/2003/340256.pdf>.